

XMM-Newton: Guest Observer Facility, Guest Observer Funding, US Instrument Team, and Education and Public Outreach

Prepared by: R. Mushotzky, NASA/GSFC, US Mission Scientist,
the US *XMM-Newton* Users Group (R. Griffiths, Chair),
and staffs of the US Instrument Team and the US *XMM-Newton* GOF

Summary

On behalf of the US *Newton X-ray Multi-Mirror Observatory (XMM-Newton)* users community, the US Instrument Team, the NASA Goddard Space Flight Center (GSFC) Guest Observer Facility (GOF), and the NASA *XMM-Newton* Education and Public Outreach (E/PO) program, we request funding for the continued support of US participation in the European Space Agency (ESA) *XMM-Newton* mission. *XMM-Newton's* instruments provide unique data enabling US astronomers to continue to produce exciting new discoveries and high-quality results, and at particularly low cost to NASA relative to other Great Observatory-class missions.

Over 1,600 astronomers, roughly 20% of the worldwide community, have participated in the *XMM-Newton* project. Continuing in the fifth Announcement of Opportunity (AO-5), the oversubscription by the community remains a factor of seven in the Guest Observer (GO) process. US astronomers has been a major participant throughout all AOs, and in AO-5, almost 40% of the accepted proposals had US Principal Investigators (PIs), and an additional 25% had US Co-investigators (Co-Is). ESA has extended the *XMM-Newton* mission for another four years, and we anticipate a similar US response and success rate in future AOs. Moreover, with over 250 refereed papers per year (128 in the most recent quarter), with a commensurate proportion led by US authors, the scientific output from *XMM-Newton* remains high, and these results are cited four times more often than the average refereed paper in the astronomical literature. This US publication rate is now close to that of *Chandra*.

XMM-Newton observations provide excellent data for the study of a wide variety of astrophysical phenomena primarily supporting NASA's goal of discovering the structure and evolution of the universe, as laid out in the 2006 NASA Strategic Plan. Below we present examples of the scientific return of *XMM-Newton*, the status of the observatory, the activities of the US instrument team, the services provided by the GOF, the proposed budget, and *XMM-Newton* E/PO activities.

Mission Overview

XMM-Newton is the second cornerstone of the ESA *Horizon 2000* program. Launched on 1999 December 10, it remains in full operation and is in excellent health. ESA mission support is confirmed until 2010 March 1, with a high probability of future extensions. As of 2006 February 28, over 4900 targets have been observed. All science data are made public after the expiration of a proprietary period, typically one year after data delivery for GO observations. The *XMM-Newton* archive had 4059 observations publicly available as of 2006 February 28. By the end of 2006 March there will be over ~ 1100 refereed papers published based on *XMM-Newton* data, with new papers appearing at the rate of nearly one per day (see Figure 1 and the publication list: http://xmm.gsfc.nasa.gov/docs/xmm/xmmhp_bibliography.html). Over the last two years *XMM-Newton* and *Chandra* have had similar numbers of refereed publications.

XMM-Newton excels in providing high throughput X-ray imaging and spectroscopy for an extremely wide variety of astrophysical sources, from comets and planets to quasars and clusters of galaxies. With all six instruments constantly observing a large field of view, the well-calibrated serendipitous source archive is proving to be a vast resource for ancillary research. However, only through the availability of *XMM-Newton*, *Chandra*, and *Suzaku* observations does the world community achieve the full complement of high angular resolution, high throughput, high spectral resolution, and low background in the 0.2–12 keV band.

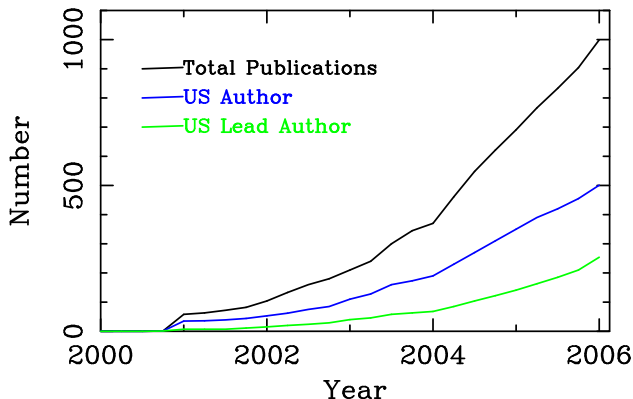


Figure 1: *XMM-Newton* publication history showing the rapid growth in the number of refereed papers.

XMM-Newton is one of the world’s pre-eminent astronomical observatories, as shown by the high proposal pressure (roughly seven times oversubscribed) and the frequent citation of refereed papers (four times the average rate). US scientists, who author 40% of the successful proposals and refereed papers, would be placed at a severe disadvantage in many areas of astrophysical research without continued US community access to *XMM-Newton*.

The science goals and achievements of *XMM-Newton* are directly responsive to the 2006 NASA Strategic Plan¹, providing unique and important data for the strategic goal of “Discovering the origin, structure, evolution, and destiny of the universe” (Sub-goals 3D1-3). *XMM-Newton* allows studies of the fundamental processes of neutron stars and black holes, the creation of the elements in supernova explosions and their dispersal in supernova remnants and starburst galaxies, the evolution of the elements on the largest scale in clusters and groups of galaxies, and the distribution of dark matter in clusters, groups, and elliptical galaxies. The study of active stars allows for direct comparison with the early solar system and star forming regions for understanding the origin and evolution of stellar systems. *XMM-Newton* has determined the positions and spectral characteristics of gamma-ray bursts, providing a high signal-to-noise (S/N) complement to *Swift*. *XMM-Newton* has examined relativistic processes from neutron stars to quasars and detected broad Fe K lines in the average spectra of the source of the X-ray background. *XMM-Newton* also provides the capability of simultaneous X-ray and optical/UV observations. While there is strong potential for overlap in the science areas of *XMM-Newton*, *Chandra* and *Suzaku*, each mission has been optimized differently in the six-dimensional space of angular resolution, band-pass, collecting area, spectral resolution, timing ability, and instrumental background. In view of the extensive proposal oversubscriptions for the three programs, the world-wide astronomical community has decided that all of these observatories are vital.

XMM-Newton observes in the 0.2–12 keV and optical/UV bands. Its large collecting area and highly elliptical orbit allow long, uninterrupted observations with

¹http://www.nasa.gov/pdf/142302main_2006_NASA_Strategic_Plan.pdf

unprecedented sensitivity. The contiguous coverage (up to ~ 135 ks) is more important now that *Chandra* is limited to ~ 60 ks or less in many orientations. The *XMM-Newton* Reflection Grating Spectrometer (RGS) provides the only high spectral resolution instrument capable of observing extended sources.

The observatory has three co-aligned high throughput 7.5 m focal length X-ray telescopes with $6''$ full width at half maximum (FWHM) angular resolution. The European Photon Imaging Camera (EPIC) charge-coupled device (CCD) detectors provide X-ray images over a $30'$ field of view. Higher resolution spectra ($E/\Delta E \sim 200 - 800$) are provided by the RGS that deflect half of the beam from two of the X-ray telescopes. The sixth instrument, the Optical Monitor (OM), is a co-aligned 30 cm optical/UV telescope sensitive in the 1600–6500 Å band. **All the scientific instruments operate simultaneously, providing exceptionally rich data sets.** The instruments can be run in a variety of modes, allowing them to be tuned for the science needs of a given observation.

The upcoming release of the 2nd *XMM-Newton* catalog will contain $\sim 10^5$ sources, a huge increase in the number of serendipitous X-ray sources which, with the availability of the *XMM-Newton* Slew Survey, Sloan digital sky survey, and other large astronomical databases, will allow a major step forward in archival research and the basis for future proposals.

1 XMM-Newton Science

XMM-Newton’s research program is peer-review driven with target of opportunity possibilities and thus it is very difficult to determine what will be the next great discovery. Every year since *XMM-Newton* was launched has seen major results across many areas of science. One way of documenting the evolving scientific program is via the accepted large projects. Starting in AO-3 these have focused on clusters of galaxies, monitoring of the galactic center, a large solid angle deep X-ray survey, and a survey of the Taurus molecular cloud. AO-4 brought projects to study the intergalactic medium, timing observations of ultra-luminous X-ray sources, time variability of AGN Fe lines, and the spin rate of an isolated neutron star. In AO-5 there is a deep and wide survey of M31, a follow-up of *Swift* BAT sources, a very large but relatively shallow X-ray survey in the SWIRE field to search for large scale structure, measurement of the ionization structure of “dipping” X-ray sources, and a study of the relativistic double pulsar PSR J0737-3039. Many of the recent results of *XMM-Newton* were presented at the The X-ray Universe 2005 meeting held in 2005 September in Spain and attended by over 300 researchers and with over 850 authors on the 384 invited and contributed papers (see <http://www.congex.nl/05a11/> for the abstracts). *XMM-Newton* is also well represented at many other international and national astronomical meetings.

The future science of *XMM-Newton* will be considerably enhanced by the availability of the 2nd *XMM-Newton*, Slew Survey, and OM catalogs, which will provide “finding charts” for future proposals and large samples of all types of objects. These databases will enable not

only direct archival research but also new GO programs. The phase space for discovery with *XMM-Newton* has increased rather than decreased through the years and that there are many rich and varied science areas to study. Continual improvements in calibration and the advent of new software will allow diffuse background studies and measurement of the mass profiles of clusters. The continued development of the basic science analysis system (SAS) has made analysis easier and more robust as well as providing new automatic data products, easing the analysis of the large and complex data sets. We believe that the best is yet to come from *XMM-Newton*!

The wealth of *XMM-Newton* results requires a focus on a small number of some of the representative results. With more than 1400 accepted GO proposals and more than 1100 refereed papers, the breadth and depth of science is representative of a “Great Observatory.” The following is a taste of what has been accomplished and suggests what the future might hold.

1.1 Active Galactic Nuclei (AGN)

XMM-Newton observations of AGN continue to provide the highest quality spectral and timing data crucial for understanding the origin of the continuum and the nature and distribution of matter near the black hole.

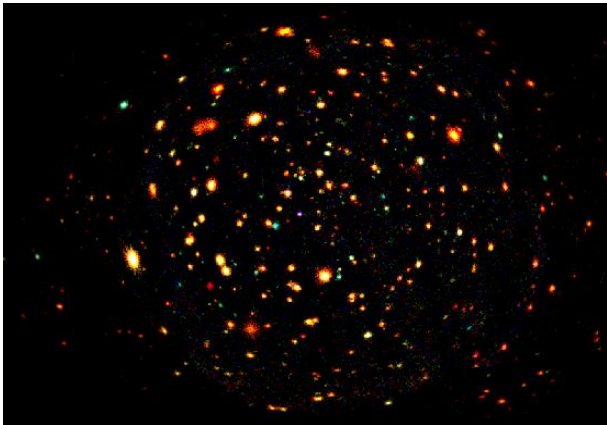


Figure 2: Color composite image of the ~ 800 ks *XMM-Newton* image of the Lockman Hole from Hasinger (2004). The image was obtained combining three energy bands: 0.5-2 keV, 2-4.5 keV, 4.5-10 keV (respectively red, green and blue).

Hasinger et al. (2005) and Streblyanska et al. (2005) used a deep EPIC observation of the Lockman hole (Figure 2) to derive the average X-ray spectra of a large sample of AGN with optical identifications. A broad Fe $K\alpha$ line, consistent with the relativistically broadened lines seen in individual spectra of brighter sources is present in both type I and type II objects, but the profiles of the two classes differ significantly. The composite profile for the type I objects is consistent with emission from gas near a spinning black hole (Laor 1991). This provides a strong confirmation of the existence of broad Fe K lines in general and for the generation of the line from regions near the event horizon.

The high throughput of *XMM-Newton* has allowed the direct detection of changes in the shape of the Fe K

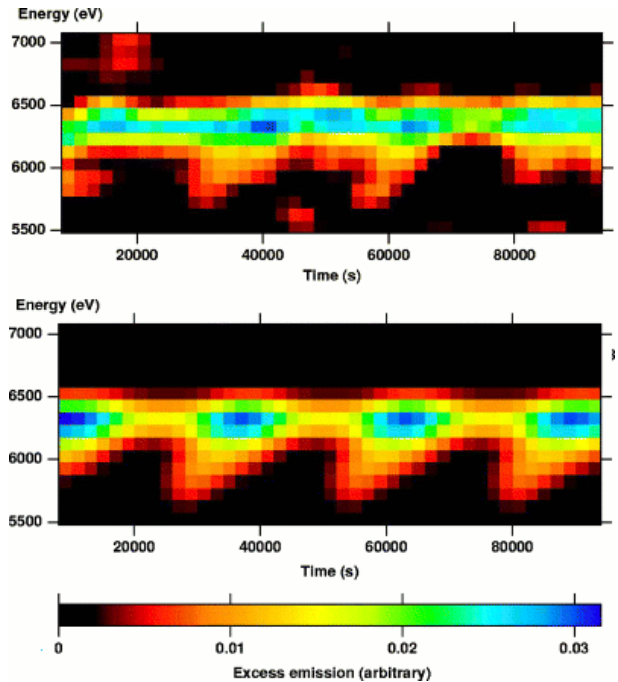


Figure 3: *Upper panel:* The NGC 3516 iron K region displayed in time and energy from EPIC data. *Lower panel:* Theoretical model of Fe emission from gas in Keplerian rotation near a black hole (Iwasawa et al. 2004).

emission line on short timescales, opening up a new field in the study of AGN. (Figure 3, Iwasawa et al. 2004, Turner et al. 2005, 2006) allowing the first direct estimates of the location of the production region, confirming its origin in regions close to the event horizon and an estimate of the black hole mass. A complementary study (Risaliti et al. 2005) has detected time variable absorption lines between 6.7-8.1 keV at high significance. These features are due to Fe XXV and Fe XXVI $K\alpha$ and $K\beta$ lines, outflowing with velocities varying between ~ 1000 and ~ 5000 km s^{-1} . The high equivalent widths ($EW_{rmK\alpha} \sim 100$ eV) and the $K\alpha/K\beta$ ratios imply that the lines are due to absorption of the AGN continuum by a highly ionized gas with column density $N_H \sim 5 \times 10^{23}$ cm $^{-2}$ at a distance of $\sim (50-100)R_S$ from the black hole, where R_S is the Schwarzschild radius.

The bright Seyfert 1 MCG-6-30-15 showed complex variability of the flux and the continuum shape (Vaughan & Fabian 2004), consistent with a variable component, identified as the primary power law, and a constant reflection continuum. Both components originate near the black hole and the spectra and time series are highly distorted by effects due to strong gravity (Fabian & Miniutti 2005). These results showcase the power of *XMM-Newton* to probe the innermost regions around supermassive black holes. Similar results have been seen in NGC4051 (Ponti et al. 2006) indicating that general relativistic effects may be more prominent than previously believed.

The broad-band high signal to noise *XMM-Newton* spectra have revealed the common presence of a soft “excess” in most type I AGN (Piconcelli et al. 2005) which can be fit by a low temperature black body independent of

the luminosity of the AGN or the mass of the black hole. This has challenged models of the formation of the low energy continuum (Gierlinski & Done 2004) indicating that the soft continuum maybe be due to reprocessing in either the accretion disk or a relativistic wind.

On kpc scales, *XMM-Newton* has provided strong clues to the origin of the observed radio structures in FRI and FRII radio galaxies (Croston et al. 2005). In FRIs, the distribution of hot gas determines the radio-lobe morphology and the subsonic expansion of the lobes heats the surrounding gas. In FRIIs, the EPIC images demonstrate that the sources are in equipartition and in pressure balance with their environment. These *XMM-Newton* observations provide information about the heating mechanisms used to transfer energy from the radio sources to the gas (e.g., Worrall et al. 2005) and on the physical parameters in the radio structures (Sambruna et al. 2004).

1.2 Clusters of Galaxies

Cluster studies with *XMM-Newton* provide critical tests of the predictions of the fundamental paradigm of large-scale structure formation, gravitationally-driven structure growth, galaxy formation and evolution models, the physics of heating and cooling, and the processes driving the hydrodynamics of the intracluster medium.

1.2.1 *XMM-Newton* Cluster Physics and Cosmology

Spatially resolved X-ray spectroscopy allows the derivation of radial profiles of temperature, gas density, and mass. The comparison of mass profiles with the predictions of the cold dark matter models (the so-called NFW mass profiles) and cosmological simulations can be done directly at the mass scale of clusters of galaxies. There is a debate about whether or not the mass profiles of clusters out to $\frac{1}{2}$ of the virial radius are consistent with the simulations. For example, while the mass profiles of 10 clusters in Pointecouteau et al. (2005) are consistent with an NFW mass profile between $0.01 - 0.5 R_{200}$ (where R_{200} is the radius inside which the mean density is 200 times the critical density, an approximation for the virial radius), Sanderson et al. (2005) concluded that the mass profile of Abell 478 is significantly flatter than an NFW profile. The Pointecouteau et al. (2005) sample shows similarity between the scaled mass profiles and provides direct evidence for universal mass scaling in clusters and that the Λ CDM predictions of the concentration factor and mass scaling agree with the observations.

The behavior of the quantity $K = kTn_e^{-2/3}$, directly related to the “entropy”, reveals the on-going heating in the core of the cluster where the cooling times are short and the fossil evidence of previous heating at radii where the cooling times are long. The entropy distribution of a cluster determines the relationship between the X-ray luminosity of the ICM and its mean temperature, which is in turn related to the history of feedback and the shape and depth of the gravitational potential well.

There were two major entropy profile papers from *XMM-Newton*, Piffaretti et al. (2005) and Pratt et al. (2006), covering 23 objects. The $T^{2/3}$ scaled entropy profiles have remarkably similar shapes outside of $0.1R_{200}$, and

while this scaling is not what would be predicted from pure gravitational infall (self-similar) models, the slope of the entropy vs. radius is consistent with gravitational heating.

The majority of clusters, particularly at large redshift, can only be characterized by their X-ray luminosity, mean temperature, and redshift. The imprint of feedback and gravitational scaling is then read from the relationship between L_x , T_x , and z , and occasionally M_{gas} . Maughan et al. (2006) quantified these relations for 11 high-redshift clusters ($z = 0.6 - 1$), to look for evolution and found that the properties of clusters reflect the properties of the Universe at the time of their formation. The metallicity, gas fractions, and the slopes of X-ray surface brightness profile have not changed since $z \sim 1$. Kotov & Vikhlinin (2005) measured the masses, L_x , and T_x of clusters at, $z = 0.4 - 0.7$, with *XMM-Newton* and found a very low scatter in the $L-T$ relation, with an evolution of this relation consistent with the power law slope of -1 predicted by self-similar, gravitationally driven models for structure formation.

The temperature and entropy profiles of eight X-ray groups in Mahdavi et al. (2005) showed, despite their morphological differences, remarkably self-similar pressure profiles. This suggests that the underlying dark matter is also self-similar. Unlike the clusters, the asymptotic slopes of the entropy profiles appear to be significantly flatter than predicted from gravitationally driven structure formation. *XMM-Newton* is being used to probe the interesting regime between where gravitation dominates and where heating, including feedback heating, may dominate.

1.2.2 Bubbles, Shocks, Toil and Trouble in Cluster Cores

One important *XMM-Newton* result was that the individual lines in soft X-ray spectra of the centers of clusters of galaxies showed significantly less cooling than was inferred from earlier X-ray observations with lower spectral resolution (e.g., Peterson et al. 2003).

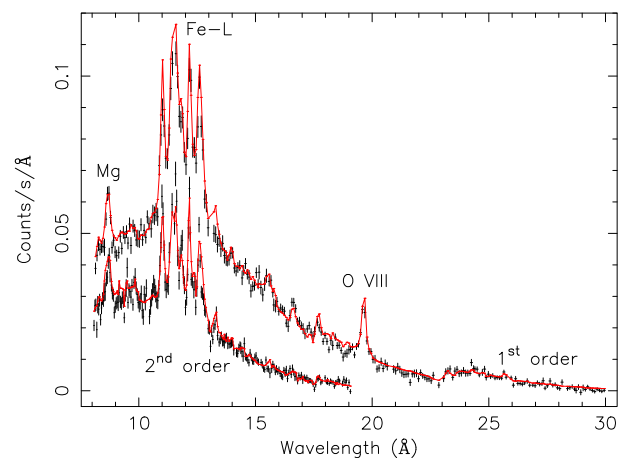


Figure 4: The RGS spectrum from the core of the cluster 2A0335+096, fit with a power-law distribution of temperatures. Weak Fe XVII and Fe XVIII lines are seen between 15-18Å, implying the presence of some cooler gas (Werner et al. 2006).

However, longer observations of these systems demonstrate that cooling flow clusters are indeed cooling, albeit at a much lower rate than expected (Figure 4). Morris & Fabian (2005) detected the Fe XVII line at 15-17 Å, emitted from gas at 0.3 keV, in the cooling flow cluster Abell 2597 in a 125 ks *XMM-Newton* RGS observation. They found cooling rates of 100 solar masses per year cooling from $T = 4$ keV.

The “cool-core” clusters also present evidence of a possible counter-cooling (heating) culprit in the form of bubbles and large-scale shocks due to a central AGN. Forman et al. (2005) using very long Chandra and *XMM-Newton* observations of M87 obtained evidence for repetitive outbursts with cavities near the jets and rings of enhanced emission at larger distances. Shallow cavities at still larger radii may be the remnants of earlier outbursts. More generally, Croston et al. (2005) found evidence for radio-source heating in low-redshift groups from the scatter in the $L - T$ relation.

1.2.3 *XMM-Newton* Cluster Surveys

The search for high-redshift clusters and groups is producing exciting results, identifying numerous groups at $z > 0.2$ and clusters at $z > 1$. Mullis et al. (2005) discovered the most distant X-ray cluster ($z = 1.4$), and the ease with which this result was obtained portends many such results to follow. Andreon et al. (2005) have found 19 *XMM-Newton* cluster candidates with very faint optical identifications. Of these six are spectroscopically confirmed high redshift ($z > 0.8$, half at $z > 1$) clusters and 3 photometrically confirmed high redshift clusters. Finally, preliminary results from the 2nd *XMM-Newton* catalog find numerous $z > 1$ cluster candidates.

The nature of groups at $z > 0.2$ is very poorly known. Willis et al. (2005), find that low-luminosity groups and clusters at $z < 0.6$ are brighter than expected, thus probing a regime of cluster luminosities and redshifts that were unavailable heretofore.

1.2.4 Galaxies in Clusters

Recent *XMM-Newton* results show direct evidence that gas rich galaxies are stripped as they move through the hot intracluster medium (ICM). Sun et al. (2006) found a long, tidally stripped tail behind a galaxy falling through the cluster Abell 2627. Another wake was reported by Sakelliou et al. (2005) behind 4C 34.16, an elliptical galaxy which has lost a substantial fraction of its mass by crossing the central regions of a cluster. Machacek et al. (2005) detected a tail between two galaxies in the Pavo Group.

Hicks & Mushotzky (2005) quantified star formation rates in cooling flow clusters in a pilot study using UV *XMM-Newton* Optical Monitor data. They discovered that in a few clusters the inferred cooling rates and star formation rates are similar, confirming previous ground based results and setting the stage for a large scale survey of star formation in cooling flow clusters.

1.3 Diffuse X-ray Emission in Galaxies

1.3.1 Planetary Nebulae

The X-ray emission in planetary nebulae (PNe) is produced by the interaction between a current shocked fast

stellar wind and the progenitor’s mass loss during the AGB phase. X-ray emission has been detected from young elliptical and bipolar PNe, but not from evolved PNe. The *XMM-Newton* X-ray spectra of PNe are better fitted by models with nebular abundances than with stellar wind abundances, (Gruendl et al. 2006) indicating that significant mixing of cool nebular material has taken place. This nebular mixing explains the extremely low plasma temperatures observed in evolved PNe.

1.3.2 Superbubbles

Superbubbles are large interstellar shell structures formed as a result of stellar energy feedback from a large number of massive stars, and are expected to be filled with hot gas and exhibit diffuse X-ray emission. *XMM-Newton* observations of superbubble 30 Dor C and N51D in the Large Magellanic Cloud have shown that the amount of thermal energy is lower by a factor of a few than expected from standard models. More surprisingly, the diffuse X-ray emission from both 30 Dor C and N51D possess a power-law component in addition to the thermal component (Cooper et al. 2004; Smith & Wang 2004) whose origin is not understood.

The expansion of superbubbles may trigger star formation. A color composite (Figure 5) of N51D in X-ray, $H\alpha$, and $8 \mu\text{m}$ images clearly reveals that the dust globules are surrounded by the hot gas in the superbubble interior. The thermal pressure of the hot gas derived from the *XMM-Newton* observations is comparable to the thermal pressure in the ionized superbubble shell, but lower than the pressure in the ionized surface of the dust globule. The hot gas is responsible for driving the expansion of the superbubble (Chu et al. 2005).

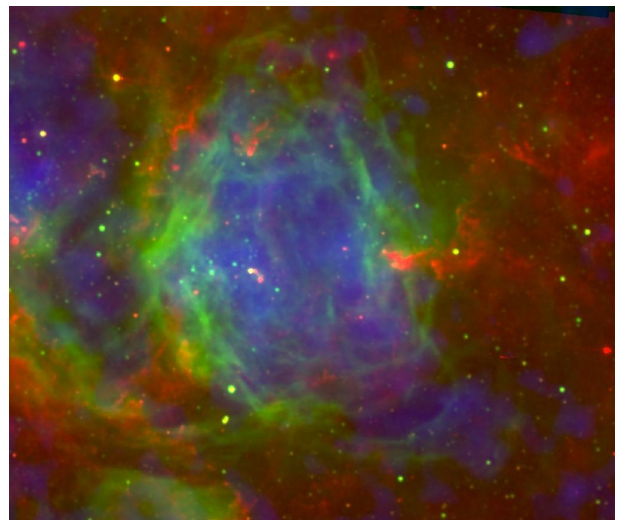


Figure 5: Color composite images of the superbubble N51D in the Large Magellanic Cloud. The $H\alpha$ emission is displayed in green, X-ray emission in blue, and $8 \mu\text{m}$ emission in red.

1.3.3 LMC Supernova Remnants

XMM-Newton’s high sensitivity allows the study of large, evolved supernova remnants (SNRs) in nearby galaxies. SNR 0450-70.9, with a size of $100 \text{ pc} \times 70 \text{ pc}$, is the largest SNR known and the temperature and den-

sity derived from X-ray spectral fits show that the interior is still overpressured and drives the SNR expansion (Williams et al. 2004). The DEML 316 SNR contains two shells, and the abundances determined from the X-ray spectra suggest that the northeast shell is a remnant of a Type Ia supernova and the southwest shell is a remnant of a type II supernova (Williams & Chu 2005).

1.4 Galaxies

XMM-Newton allows the study of binaries in external galaxies in a similar fashion to studies of Milky Way binaries two decades ago, allowing significant breakthroughs in discovering new classes of objects and testing what we have learned from local objects.

1.4.1 X-Ray Binaries in Other Galaxies

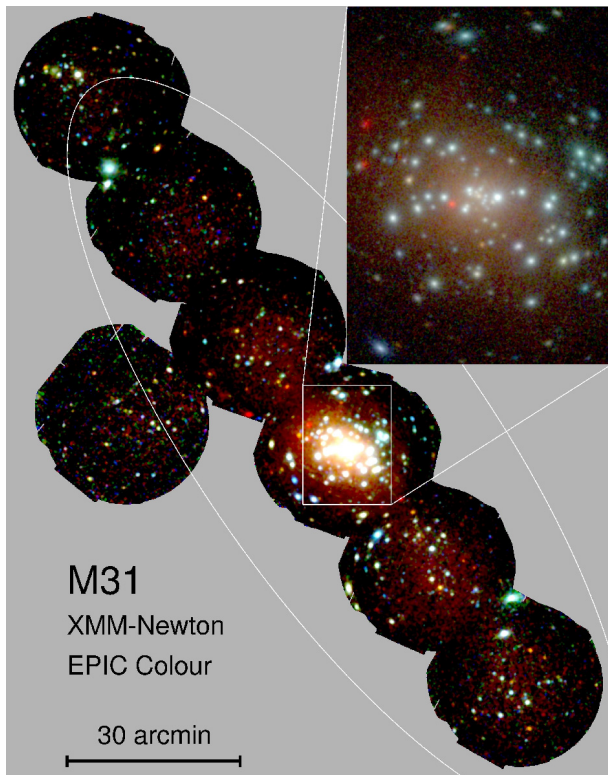


Figure 6: *XMM-Newton* mosaic of M31 (Pietsch et al. 2005).

A survey of M31 (Figure 6) studied the X-ray point source population (Pietsch et al. 2005). 856 sources were detected over 1.24 deg^2 down to a luminosity of $4 \times 10^{34} \text{ ergs s}^{-1}$, and the first X-ray bursts outside the Milky Way were detected (Pietsch & Haberl 2005). These two type I X-ray bursts demonstrate that *XMM-Newton* observations can be utilized to classify neutron star low mass X-ray binaries in Local Group galaxies.

Kong & DiStefano (2003) monitored an outburst of a supersoft X-ray source in NGC 300 and studied the spectrum and its evolution. The detection of a 5.4 hr periodicity in the low state combined with the high luminosity and soft spectrum of the source argue that it is a black hole X-ray binary.

1.4.2 Ultra-luminous X-ray (ULX) sources

The ultraluminous X-ray sources in nearby galaxies (Miller & Colbert 2004) are either black holes of $M > 100 M_{\odot}$ or have a type of accretion not known to occur in the Milky Way. The best constraints on their nature comes from the comparison of their X-ray spectra and timing behavior with the better understood AGN and galactic black holes (GBHs). *XMM-Newton* data provide the best constraints on these properties.

Two surveys of high signal to noise X-ray spectra (Winter et al. 2005, Feng & Kaaret 2005) confirmed the discovery by Miller et al. (2004) and Wang et al. (2004) that many of the ULX spectra can be fitted by the same models used to describe GBHs in the high state, a steep power law and a black body, but with a much lower temperature for the black body component than in GBHs. The spectra of the less luminous ULX population can be well described by a flat power law similar to GBHs in the low state. Since the low state is observed when the object is radiating at less than 10% of the Eddington limit the observed luminosity can be used to estimate the mass. The deep *XMM-Newton* observation of the ULX in M82 (Dewangan et al. 2006) has discovered the existence of both a QPO and a break in the power density spectrum (PDS). Extensive modeling of GBHs PDS and spectra results in a mass estimate of $25\text{-}520 M_{\odot}$. However, a similar high S/N observation of the ULX in Holmberg II (Goad et al. 2006) failed to find any power in the PDS, a behavior very different from any galactic analog. Detailed modeling of the X-ray spectra of Holmberg II X-1 combined with *HST* data (Kaaret et al. 2004) have confirmed that the source is not beamed and it is truly ultraluminous.

1.4.3 Young Supernovae

SN 1979C, one of the oldest observed X-ray emitting supernovae (Figure 7, Immler et al. 2005), is still radiating at a high X-ray luminosity, ($L_{0.3-2} = 8 \times 10^{38} \text{ ergs s}^{-1}$), showing no sign of a decline over a period of 16–23 yrs after its outburst. This behavior is caused by the interaction of the SN shock with dense circumstellar matter (CSM), deposited by a strong stellar wind from the progenitor with a mass-loss rate of $\dot{M} \approx 2 \times 10^{-4} M_{\odot} \text{ yr}^{-1}$. The X-ray data imply a strongly decelerated shock and a constant progenitor mass-loss rate and wind velocity over the past > 16,000 yrs of the progenitor. The SN is detected in the optical/UV with the OM, with *B*, *U*, and *UVW1*-band luminosities of 5, 7, and $9 \times 10^{36} \text{ ergs s}^{-1}$, respectively, caused by the strong interaction of the SN shock with dense CSM.

The X-ray light curve of the Type II SN 1986J (Temple et al. 2005) in NGC 891 declines as $L_X \propto t^{-2}$, significantly steeper than expected from circumstellar interaction with a stellar wind profile.

1.5 Supernova Remnants and Neutron Stars

As extended objects with high temperatures and a complex set of abundances and ionization conditions, supernova remnants (SNRs) are prime objects for study with *XMM-Newton*. Spatially resolved SNR spectra separate thermal from non-thermal emission, identify stratification of ejecta, separate the forward and reverse shock

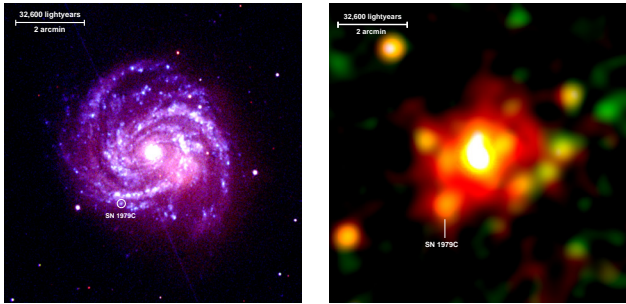


Figure 7: Left-hand panel: *XMM-Newton* optical/UV image of the galaxy M100 and SN 1979C obtained with the Optical Monitor in the *B*, *U*, and *UVW1* filters. The position of SN 1979C is marked by a white circle. Right-hand panel: Composite *XMM-Newton* X-ray image of the galaxy M100 in soft (0.3–1.5 keV, red), medium (1.5–4 keV, green) and hard (4–10 keV, blue) X-rays. The image shows large amounts of diffuse X-ray emission from hot gas in the galaxy (red), various point-like X-ray sources and SN 1979C south-east of the nucleus of M100 (Immler et al. 2005).

regions, measure variations in temperature and ionization conditions, and identify pulsar wind nebulae. The large effective area and good angular resolution of *XMM-Newton* provide rich spectra on physically important spatial scales.

1.5.1 Non-thermal Emission from SNRs

A new class of SNRs, dominated by non-thermal emission may be primarily responsible for the acceleration of cosmic rays up to energies of 10^{15} GeV. *XMM-Newton*, with its large collecting area and good PSF up to 10 keV, is ideally suited for studying this emission in detail. Rothenflug et al. (2004) used the deep *XMM-Newton* image and high-quality spectra of SN 1006 to measure the azimuthal and radial variations in the non-thermal emission produced by the highest energy electrons. They measured the cutoff frequency for these electrons and determined that the number density and maximum energy must be highest at the bright limbs of the remnant (Figure 8), supporting a “polar cap” geometry model as opposed to an “equatorial” model. G 347.3-0.5, another member of this class, exhibits a more complicated morphology, and *XMM-Newton* observations (Cassam-Chenai et al. 2004, Hiraga et al. 2005) strengthened the case for an interaction between the remnant and nearby molecular clouds, providing an explanation for the distortions from a shell-type morphology. The synchrotron spectrum is steepest in the faint, central regions and flattest near the edges (the presumed location of the shock). These data place a stringent upper limit on any thermal emission component and suggest that the remnant is closer than previously believed (1.3 kpc instead of 6.0 kpc).

In the newly-discovered SNR along the line of sight to the Vela SNR (“Vela Junior”), deep *XMM-Newton* observations detected a weak emission feature at 4.45 keV due to ^{44}Ti (Iyudin et al. 2005). The presence of this short-lived isotope implies that G266.2-1.2 is a very young SNR, perhaps even younger than Cas-A.

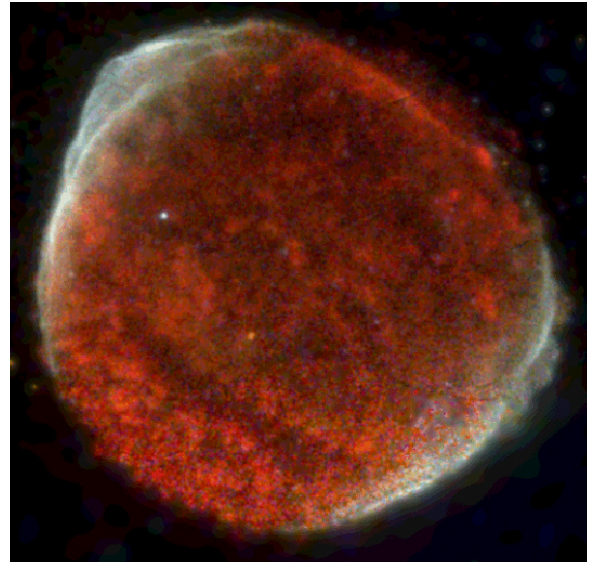


Figure 8: Three color image of SN 1006 (Rothenflug et al. 2004). The red, green, and blue channels are 0.5 to 0.8 keV, 0.8 to 2.0 keV, and 2.0 to 4.5 keV, respectively. The areas dominated by non-thermal emission appear white and the areas dominated by thermal emission appear red.

1.5.2 SNR Interaction with the Interstellar Medium

SNe produce the heavy elements and SNRs distribute these elements throughout the interstellar medium (ISM). The shock waves of SNRs disturb and compress the material in the ISM. *XMM-Newton* has provided detailed spectral data which allow the study of these shock/cloud interactions. A classic example of a massive star exploding near the molecular cloud complex from which it formed and then interacting with that cloud complex is the galactic SNR CTB 109 (see Figure 9). The *XMM-Newton* observations (Sasaki et al. 2004) have confirmed that all of the bright emission associated with the shell is completely thermal and has abundances consistent with swept-up ISM. The spectra from the bright interior feature known as the “Lobe” is also completely thermal but has enhanced Si abundances, the first detection of SN ejecta in CTB 109.

1.5.3 Neutron Stars

The past decade has revealed a wide variety in the birth states of neutron stars (NS) producing a large number of classes viz: Compact Central Objects (CCOs), Anomalous X-ray Pulsars (AXPs) or Magnetars, Transient AXPs (TAXPs), Isolated Neutron Stars (INS), and X-ray Dim INS (XDINS), and, presumably, Soft Gamma-ray Repeaters (SGRs). *XMM-Newton*’s timing and phase-resolved spectroscopy capabilities have been crucial in determining the characteristics of these new objects and refining the class definitions

1.5.3.1 CCOs and AXPs

CCOs are defined by their association with SNRs, mostly steady flux, lack of radio or optical counterparts, thermal emission, and absence of a pulsar wind nebulae. Timing observations of the CCO in the SNR Kes 79 (Gotthelf et al. 2005) discovered pulsations with

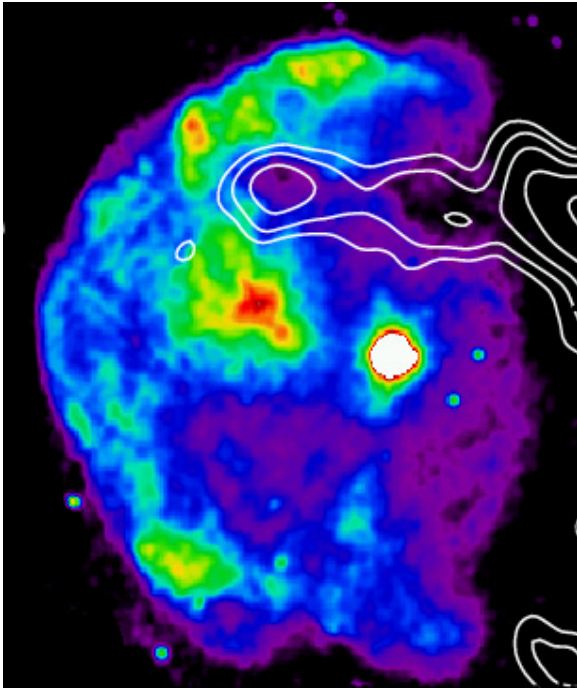


Figure 9: *XMM-Newton* image of CTB 109 in the 0.3-4.0 keV band with the CO contours overlaid (Sasaki et al. 2004). The bright source near the center of the semicircle is the AXP 1E 2259+586. The molecular cloud complex is located to the west. The bright diffuse feature just east of the pulsar is the “Lobe”.

a 105 ms period, only the second detection of X-ray pulsations from a CCO. The newly detected pulsar has spin properties typical of rotation-powered pulsars, but an X-ray temperature and luminosity considerably higher. However, its inferred magnetic field and X-ray luminosity are significantly lower than the AXPs. This discovery is a crucial step in linking CCOs, AXPs, and rotation-powered pulsars in a continuum of characteristics.

AXPs can be remarkably steady in their X-ray luminosity and then suddenly experience an outburst or a flare. The newly-discovered AXP XTE J1810-197 went into an outburst state in 2003 and has been declining since. Halpern & Gotthelf (2005) modeled the *XMM-Newton* spectrum with two blackbody components with temperatures of 0.25 and 0.67 keV and found that these components were decreasing exponentially with time constants of $\tau_1 = 900$ days and $\tau_2 = 300$ days, respectively. This source is the second possible identification of a TAXP. Gotthelf et al. (2004) suggest that TAXPs, AXPs, CCOs, and SGRs may all be a single class of objects in various stages of evolution, but with the same underlying process responsible for their X-ray emission.

The first detection of pulsations from a member of a small but growing class of young radio pulsars with magnetic fields of a few $\times 10^{13}$ G (Gonzalez et al. 2005) gives a characteristic age of 1700 yr and an inferred magnetic field of 4.1×10^{13} G. The pulsed spectrum is well-fitted by a blackbody model with $kT = 0.20$ keV and emitting surface of 3.4 km. This makes PSR J1119-6127 the youngest pulsar from which thermal X-ray emission has been detected.

1.5.3.2 Isolated Neutron Stars (INS)

The current atmosphere models of INS predict spectral lines in the X-ray bandpass, hence it came as a surprise that early observations of the 3 brightest of these objects showed no spectral features. However, broad *absorption* features were found in the spectrum of 1E 1207.4-5209 and they vary with pulse phase (Mereghetti et al. 2002 and Bignami et al. 2003). In the last few years, *XMM-Newton* observations have revolutionized this field by detecting broad absorption features which vary in time, not only with pulse phase but also long-term variations related to the state of the source. Haberl et al. (2003) detected broad absorption features in RX J1308.6+2127 which varied with pulse phase. Similar features were detected in three other INS’s (van Kerwijk et al. 2004, Haberl et al. 2004, and Zane et al. 2005). The explanations for these features, include proton and/or electron cyclotron lines and atomic transition lines. If the cyclotron line explanation is correct, it implies high magnetic fields, on the order of 10^{13} G, contrary to expectations. Vink et al. (2005) reported that RX J0720.4-3125’s blackbody temperature and depth of the absorption feature have both reversed their increase with time and are starting to decrease. The study of the absorption features in these isolated, nearby NS is just beginning and promises to produce new insights into the atmospheres and the emission from the surface of neutron stars.

1.6 XRBs and CVs

1.6.1 X-Ray Binaries in the Milky Way and Magellanic Clouds

The large collecting area of *XMM-Newton* provides high-S/N, high-resolution spectroscopy of galactic X-ray binaries. Juett & Chakrabarty (2005) have studied the spectra of ultracompact X-ray binaries thought to have hydrogen deficient or degenerate donor stars. They discovered that the companions are Ne-rich with circumstellar material with unusually high metal abundances. The strengths of the circumstellar absorption lines vary due to changes in the ionizing flux of the stars. *XMM-Newton* data have also measured strongly skewed Fe K lines in GX 339-4 and other black hole candidates (Miller et al. 2004), similar to that seen in AGN, strongly arguing for a best-fit inner disk radius of $(2 - 3)r_g$ and suggesting that GX 339-4 harbors a black hole with $a \geq 0.8 - 0.9$ (where $r_g = GM/c^2$ and $a = cJ/GM^2$). Hicox et al. (2004) showed that the soft excess in X-ray binaries is extremely common and is almost certainly due to reprocessing of hard X-rays from the neutron star by the inner region of the accretion disk. In another analogy to AGN, Díaz-Trigo et al. (2006) used RGS data to determine that the soft X-ray spectrum of the X-ray “dippers” is caused by a highly ionized absorber, solving a 20 year old problem.

1.6.2 Cataclysmic Variables (CVs) and Related Objects

Cataclysmic variables (CVs) are typically faint X-ray sources with X-ray luminosities in the range $10^{31} - 10^{33}$ erg s^{-1} . Thus *XMM-Newton* is needed in order to obtain observations of the brighter CVs at high time resolution and spectra of the fainter CVs at high S/N.

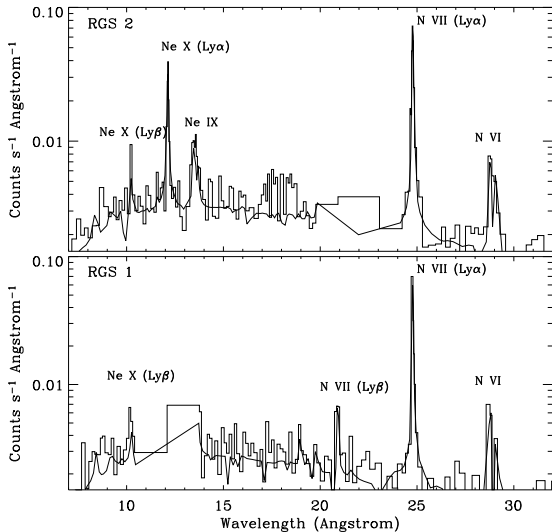


Figure 10: RGS spectra of GP Com. The strongest detected feature is the Ly α line of hydrogenic nitrogen (N VII) at 24.78 Å, but other lines of nitrogen are also present (Strohmeier 2004).

Strohmeier (2004) detected emission lines from H- and He-like ions of N and Ne from the ultracompact binary white dwarf GP Com (Figure 10). The RGS spectra indicate that the lines are emitted from a dense, hot, collisionally ionized plasma, confirming the deficiency of carbon and oxygen and obtaining the accretion rate. They conclude that the X-rays are emitted from an optically thin boundary layer around the accreting white dwarf. Pandel et al. (2005) have carried out a survey of dwarf novae in quiescence using EPIC. The spectra are in spectacular agreement with a model of an isobaric cooling flow, indicating that the X-rays originate in a cooling plasma settling onto the surface of the white dwarf, a confirmation of models for accreting white dwarf boundary layers.

1.7 Stars and Planets

1.7.1 Jupiter

XMM-Newton observations of Jupiter (Branduardi-Raymont et al. 2005) can be modeled with a combination of unresolved emission lines of highly ionized oxygen (O VII and O VIII) and a pseudo-continuum due to the superposition of many weak lines. This confirms that Jupiter’s auroral emissions originate from the capture and acceleration of solar wind ions in the planet’s magnetosphere, followed by charge exchange. The X-ray flux of the North Spot is modulated at Jupiter’s rotation period. In addition, both aurorae have a higher energy component (3 – 7 keV) due to electron bremsstrahlung. This is variable in flux and spectral shape during the 2003 November observation, which corresponded to an extended period of intense solar activity. Emission from the equatorial regions of Jupiter’s disk was also observed, with a spectrum consistent with solar X-rays scattered in the planet’s upper atmosphere. RGS spectra have resolved the prominent O VII contribution of the aurorae from the O VIII, Fe XVII and Mg XI lines originating in the low-latitude disk regions of the planet.

1.7.2 X-ray emission from Pre-Main-Sequence Stars

Hard X-ray (2 – 10 keV) emission associated with deeply embedded, very young stars is due to magnetic processes even on these youngest pre-main-sequence stars. Simon & Dahm (2005) found one embedded ($A_V \geq 10$ mag) source in NGC 2264 that has a coronal temperature over 100 MK and another that reached 140 MK during a flare. Hamaguchi et al. (2005) detected sources in CrA with temperatures of $\sim 3 - 4$ keV that are hidden by up to 180 mag. of visual extinction.

1.7.3 Accretion and X-rays from Young Stars

A crucial question addressed by *XMM-Newton* is the role of accretion in young stars. The high electron densities, unusual patterns of elemental abundances, and the low temperatures in some of these objects are all indicative of accretion rather than what is expected from typical stellar coronal X-ray emission. The first discovery of X-rays associated with accretion is from the low mass classical T Tauri star TW Hya (Stelzer & Schmitt 2004). Ness & Schmitt’s (2005) *XMM-Newton* grating observations confirm that accretion is playing a major role in the X-ray production on this star. Other examples include the young A star β Pic (Hempel et al. 2005) and the classical T Tauri star BP Tau (Schmitt et al. 2005). However this is not the general case since Argiroffi et al. (2005) found a typical (10^7 K) coronal structure for TWA 5, a coeval sibling of TW Hya. Hot ($kT \geq 3$ keV) emission was even observed from the intermediate mass Herbig Ae star HD104237 by Skinner et al. (2004).

Two low-mass T Tauri stars in Orion were observed during large optical/IR outbursts when the mass accretion rate from the disk onto the star increased dramatically. Grosso et al. (2005) found that the X-ray flux of V1647 Ori had increased by a factor of more than 100 over its level prior to the accretion outburst and showed significant short term (hour time scale) variability. In contrast, Audard et al. (2005) found that an optical outburst of V1118 Ori produced almost no increase in the X-ray flux.

1.7.4 Coronal Flaring on Low Mass Stars

XMM-Newton observations allow simultaneous observations of the X-ray emission at grating resolution with the RGS, at high time resolution with the EPIC cameras, and in the ultraviolet with the OM. These rich datasets allow detailed studies of the flare behavior and sophisticated modeling of flaring magnetic loops. An excellent example (Güdel et al. 2004) is the 65 ks observation of the M dwarf flare star Proxima Cen, which showed flaring on all the time scales sampled and the presence of flaring loops with characteristic sizes of $\sim 1 R_*$.

During a 5 ks flare on the M dwarf AT Mic, Mitra-Kraev et al. (2005b) detected a flare loop oscillation with a period of 750 s and an exponential damping time of ~ 2000 s. The oscillation is a standing magneto-acoustic wave, most likely a longitudinal slow-mode wave, with a local magnetic field strength of 105 G and a loop length of 2.5×10^{10} cm. This is the first detection of a stellar X-ray flare oscillation. The correlation between X-ray and UV flares, supports the chromospheric evaporation flare model (Mitra-Kraev et al. 2005a), with the impulsive

phase UV emission preceding the X-ray flare peak by about 10 minutes and the X-ray light curve following the time integral of the UV light curve.

1.8 Cosmology, Surveys, and Serendipitous Science

The Science Survey Consortium (SSC) X-ray Identification (XID) program (<http://xmmssc-www.star.le.ac.uk/>) has released multi-color CCD images for many *XMM-Newton* fields with details of the identifications of sources in the fields, links to optical finding charts, optical photometry of potential counterparts and reduced optical spectra. This public release of optical follow-up data is unique to *XMM-Newton* and will continue as part of the SSC function.

The *XMM-Newton* Slew Survey (Freyberg et al. 2006) now comprises 4000 sources with exposure times of 15 s and a sky coverage of $\sim 6,000 \text{ deg}^2$. Below 2 keV its sensitivity is similar to the *ROSAT* All-Sky Survey. Above 2 keV, it is 10 times more sensitive than any previous all-sky survey. The Slew Survey will provide long-term variability data for a large sample of sources. The initial catalog is expected to be released in mid 2006 and the effort will continue to the end of the mission. The 2nd *XMM-Newton* catalog will be released soon, containing $\sim 100,000$ sources 15% of them with spectra and time series. Cross correlation with data release 4 of the Sloan Digital sky survey shows 3899 galaxies and 3207 point-like objects of which 1014 have *XMM-Newton* time series and spectra.

There have been several *XMM-Newton* surveys with the goal of determining the nature of the extragalactic source populations and their evolution with cosmic time. These include: i) the COSMOS survey of 1.4 deg^2 , covering a region surveyed with *HST*/ACS and a host of other instruments; ii) the *XMM-Newton*/Subaru deep field; iii) the *XMM-Newton* 2dF-survey; and iv) the 13H *XMM-Newton*/*ROSAT* survey. A major discovery resulting from these surveys (Figure 11) has been that the evolutionary behavior of type I AGN shows a strong dependence on X-ray luminosity (Hasinger et al. 2005). While the space density of high-luminosity AGN peaks near $z \sim 2$, similar to that of optically selected quasi-stellar objects (QSOs), the space density of low-luminosity AGN peaks at redshifts below 1. A thousand AGN were used for this analysis. The key feature of this work was the completeness of the spectroscopic and photometric identifications.

In the COSMOS survey field, 1417 sources were detected (Cappelluti et al. 2006), and a population of heavily absorbed, partially leaky or reflecting absorbers has been identified, most of which are likely to be nearby Compton-thick sources. These sources may be prototypes for the class of objects responsible for the bulk of the X-ray background in the 10–40 keV energy range (Hasinger et al. 2006; Mainieri et al. 2006). The X-ray selected AGN in the COSMOS field have been used to measure the angular auto-correlation function, determining that the bias parameter for X-ray AGN is $b = 2.5 - 4$ at $0.5 < z < 1.2$ (Miyaji et al. 2006).

From fields overlapping the Sloan Digital Sky Survey, Georgantopoulos et al. (2005) have measured the X-ray

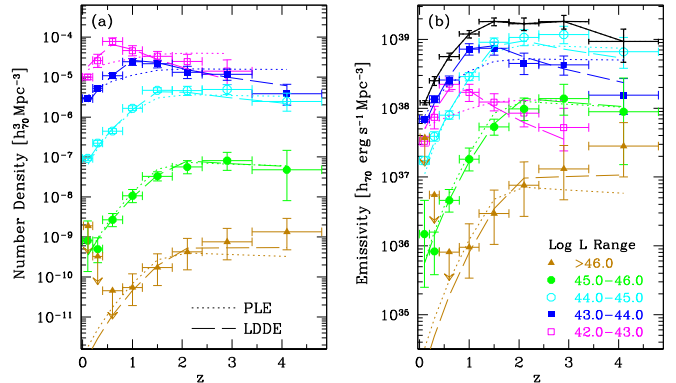


Figure 11: a) The space density of AGN as a function of redshift in different luminosity classes and the sum over all luminosities with $\log L_x \geq 42$. Densities from the PLE and LDDE models are overplotted with dashed and dotted lines. b) The same as a), except that the soft X-ray emissivities are plotted instead of number densities. The uppermost curve (black) shows the sum of emissivities in all luminosity classes plotted. (Hasinger et al. 2005)

luminosity function of normal galaxies for the first time, together with the separate luminosity functions for early and late-type galaxies.

References

- Andreon, S., et al. 2005, MNRAS, 359, 1250
Audard, M., et al. 2005, ApJ, 635, L81
Argiroffi, C., et al. 2005, A&A, 439, 1149
Bignami, G.F. 2003, Nature, 423, 725
Branduardi-Raymont, G. et al. 2005, AGUSM, P44A-02
Cappelluti et al. 2006, submitted
Cassam-Chenai, G., et al. 2004, A&A, 427, 199
Chu, Y.-H., et al. 2005, ApJ, 634, L189
Cooper, R. L., et al. 2004, ApJ, 605, 751
Croston, J. H., et al. 2005, MNRAS, 357, 279
Dewangan, G. C. et al. 2006, ApJ, 637, 21
Díaz-Trigo, M., et al. 2006, A&A, 445, 179
Fabian, A. C., & Miniutti, G. 2005, Astro-Ph/0507409
Feng, H., & Kaaret, P. 2005, ApJ, 633, 1052
Forman, W., et al. 2005, ApJ, 635, 894
Freyberg, M., et al. 2006, Astro-Ph 0512157
Georgantopoulos, I., et al. 2005, MNRAS 360, 782
Gierlinski, M., & Done, C. 2004, MNRAS, 349, 7
Goad, M. R. et al. 2006, MNRAS, 365, 191
Gotthelf, E.V., et al. 2005, ApJ, 627, 390
Gotthelf, E.V., et al. 2004, ApJ, 605, 368
Gotthelf, E.V., & Halpern, J.P.. 2005, ApJ, 632, 1075
Gonzalez, M.E., et al. 2005, ApJ, 630, 489
Grosso, N., et al. 2005, A&A, 438, 159
Gruendl et al. 2006, in preparation
Güdel, M., et al. 2004, A&A, 416, 713
Haberl, F. et al. 2003, A&A, 403, L19
Haberl, F. et al. 2004, A&A, 419, 1077
Halpern, J.P., & Gotthelf, E.V. 2005, ApJ, 618, 874
Hamaguchi, K., et al. 2005, ApJ, 623, 291
Hasinger, G. 2004, NuPhS, 132, 86
Hasinger, G., et al. 2005, A&A, 441, 417
Hasinger, G., et al. 2006, submitted
Hempel, M., et al. 2005, A&A, 440, 727
Hickox, R. C., et al. 2004, ApJ, 614, 881
Hicks, A. K., & Mushotzky, R. 2005, ApJ, 635, 9
Hiraga, J. S., et al. 2005, A&A, 431, 953
Immler, S., et al. 2005, ApJ, 632, 283
Iwasawa, K., et al. 2004, MNRAS, 355, 1073
Iyudin, A. F., et al. 2005, A&A, 429, 225
Juett, A. M., & Chakrabarty, D. 2005, ApJ, 627, 926
Kaaret, P. et al. 2004, MNRAS, 351, 83
Kong, A. K. H., & Di Stefano, R. 2003
Kotov, O., & Vikhlinin, A. 2005, ApJ, 633, 781
Laor, A. 1991, ApJ, 376, 90
Machacek, M. E., et al. 2005, ApJ, 630, 280
Mahdavi, A., et al. 2005, ApJ, 622, 187
Mainieri, et al. 2006, submitted
Maughan, B. J., et al. 2006, MNRAS, 363, 509
Mereghetti, S., et al. 2002, ApJ, 581, 1280
Miller, J. M., & Colbert, E. J. M. 2004, IJMPD, 13, 1
Miller, J. M., et al. 2004, ApJ, 606, 131
Mitra-Kraev, U., et al. 2005a, A&A, 431, 679
Mitra-Kraev, U., et al. 2005b, A&A, 436, 1041
Miyaji, T., et al. 2006, submitted
Morris, R. G., & Fabian, A. C. 2005, MNRAS, 358, 585
Mullis, C. R., et al. 2005, ApJL, 623, L85
Ness, J.-U., & Schmitt, J. H. M. M. 2005, A&A, 444, L41
Pandell, D., et al. 2005, ApJ, 626, 396
Peterson, J. R. et al. 2003, ApJ, 590, 203
Piconcelli, E., et al. 2005, A&A, 432, 15
Pietsch, W., et al. 2005, A&A, 434, 483
Pietsch, W., & Haberl, F. 2005, A&A, 430, L45
Piffaretti, R., et al. 2005, A&A, 433, 101
Pointecouteau, E., et al. 2005, A&A, 435, 1
Ponti, G. et al. 2006, Astro-Ph/0602191
Pratt, G. W., et al. 2006, A&A, 446, 429
Risaliti, G., et al. 2005, ApJ, 630, 129
Rothenflug, R., et al. 2004, A&A, 425, 121
Sakelliou, I., et al. 2005, MNRAS, 360, 1069
Sambruna, R. M., et al. 2004, A&A, 414, 885 2003ApJ...590..207
Sanderson, A. J. R., et al. 2005, ApJ, 630, 191
Sasaki, M., et al. 2004, ApJ, 617, 322
Schmitt, J. H. M. M., et al. 2005, A&A, 432, L35
Simon, T., & Dahm, S. E. 2005, ApJ, 618, 795
Skinner, S. L., et al. 2004, ApJ, 614, 221
Smith, D. A., & Wang, Q. D. 2004, ApJ, 611, 881
Stelzer, B., & Schmitt, J. H. M. M. 2004, A&A, 418, 687
Streblyanska, A., et al. 2005, A&A, 432, 395
Strohmeyer, T. E., 2004, ApJ, 608, L 53
Sun, M., et al. 2006, ApJ, 637, 81
Temple, R. F., et al. 2005, MNRAS, 362, 581
Turner, T. J., et al. 2005, ApJ, 618, 155
Turner, T. J., et al. 2006, A&A, 445, 59
van Kerkwijk, M. H. et al. 2004, ApJ, 608, 432
Vaughan, S., & Fabian, A. C. 2004, MNRAS, 348, 1415
Vink, J., et al. 2005, The Astronomer's Telegram, 650
Wang, Q. D., et al. 2004, ApJ, 609, 113
Werner et al. 2006, A&A, in press
Williams, R. M., et al. 2004, ApJ, 613, 948
Williams, R. M., & Chu, Y.-H. 2005, ApJ, 635, 1077
Willis, J. P., et al. 2005, MNRAS, 363, 675
Winter, L. M. 2005, AstroPh/0512480
Worrall, D. M., et al. 2005, Astro-Ph/0410299
Zane, S., et al. 2005, ApJ, 627, 397